DOI: 10.1002/ejoc.200600240

Geometrically Homogenous Series of Covalently Linked Zinc/Free-Base Porphyrin Dimers of Varying Length; Design, Synthesis and Characterization

Thomas Ljungdahl,[a] Karin Pettersson,[b] Bo Albinsson,[b] and Jerker Mårtensson*[a]

Keywords: Bridge-mediated coupling / Cross-coupling / Donor–acceptor systems / Porphyrin

Singlet excitation energy transfer, SEET, can be mediated by a bridge, connecting an energy donor and acceptor, via a superexchange mechanism. The mediation efficiency depends on the energy difference between the first excited states of the donor and the bridge, ΔE_{DB}, as well as the donor–acceptor distance, R_{DA}. We have previously constructed a series of donor–bridge–acceptor, D–B–A, systems that allowed us to study how SEET depends on ΔE_{DB}. To expand this study into a second dimension, the distance dependence, a new series of D–B–A systems were constructed. This series was based on the same zinc/free-base porphyrin couple as the donor–acceptor pair in the previous series. Their relative orientation was also retained. In contrast to our first series, the bridges in the latter were of varying length. The bridges were oligo(phenyleneethynylene)phenylene (OPE) structures and the length was systematically changed by increasing the number of phenyleneethynylene units from 1 to 4. To obtain high quality samples, the D–B–A systems were assembled by a building block approach where the zinc and free-base porphyrins were introduced separately using Heck alkynylations. The performance of the OPE structure as a mediator and scaffold is discussed in terms of singlet excited state energies and flexibility. For the first time, when combining the topical D–B–A systems with our previous subset, a homogeneous series of D–B–A systems has been synthesized that allows for studies of both the distance dependence and the energy difference dependence of SEET.

Introduction

The covalently linked donor–bridge–acceptor, D–B–A, systems that have been prepared to study excitation energy transfer, EET, are numerous. In many of the earlier systems, the bridge was assumed to be a mere spectator in the transfer process. The systems were used to verify the dependence of EET on the different parameters that appear in the expression for EET efficiency derived by Förster[1] based on a through-space dipole–dipole interaction; e.g. the dependence on distance and relative orientation between the donor and the acceptor and the dependence on overlap between donor fluorescence and acceptor absorption. However, the value of the bridge as a mediator of electronic interaction between the donor and the acceptor, as opposed to a passive scaffold positioning the donor and acceptor at a fixed distance and relative orientation, was soon recognized. In latter systems, the mediation capacity of the bridge was therefore explored in the context of the orbital overlap dependent exchange formalism derived by Dexter[2] and the superexchange theory derived by McConnell.[3] The EET was studied with respect to the dependence on bridge length,[4–12] bridge conformation,[13] and the energy differences between the excited states of the donor and the bridge,[14] affecting the overall magnitude of the electronic donor–acceptor interaction.

Excitation energy transfer according to the exchange mechanism can be pictured as two simultaneous electron transfer, ET, processes: (1) ET from the formally singly occupied LUMO of the photoexcited donor to the empty LUMO of the acceptor and, (2) transfer of one electron from the HOMO of the acceptor to the formally singly occupied HOMO of the donor, thus generating a ground state donor and an acceptor in its first excited state. In fact, it has been shown, both experimentally and theoretically, that triplet EET is related to electron and hole transfer. In addition, ET via or through a bridge can be viewed as a quantum mechanical tunneling process in which an electron escapes from one potential minimum to another separated by an, in a classical sense, insurmountable potential barrier. According to the theory for such tunnel effect phenomena, the probability for ET will depend on the width and the height of the barrier, where the barrier width is the distance between donor and acceptor (R_{DA}) and the barrier height is the energy splitting between the relevant states of the donor and bridge (ΔE_{DB}).

[a] Department of Chemical and Biological Engineering/Organic Chemistry, Chalmers University of Technology,
41296 Göteborg, Sweden
Fax: +46-31-7723657
E-Mail: jerker@chembio.chalmers.se
[b] Department of Chemical and Biological Engineering/Physical Chemistry, Chalmers University of Technology,
41296 Göteborg, Sweden

Supporting information for this article is available on the WWW under http://www.eurjoc.org or from the author.

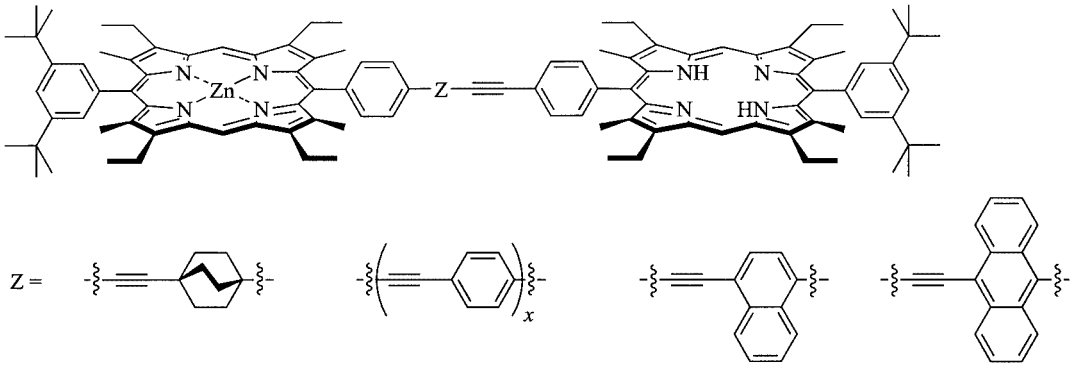

		ZnP-*n*B-H_2P:		
		ZnP-2B-H_2P: $x = 0$		
ZnP-RB-H_2P:	**ZnP-OB-H_2P**	**ZnP-3B-H_2P**: $x = 1$	**ZnP-NB-H_2P**	**ZnP-AB-H_2P**
		ZnP-4B-H_2P: $x = 2$		
		ZnP-5B-H_2P: $x = 3$		

Figure 1. An overview of the two D–B–A series designed for EET studies with the systems featuring the repeating phenylethynyl-unit being the topical series. The two series share a common member in **ZnP-3B-H_2P**.

Because exchange EET via or through a bridge can be pictured as two simultaneous ET processes and ET can be treated as an electron tunneling process, it should also be possible to treat exchange EET as a tunneling phenomenon. The probability for electron exchange shows exponential distance dependence as well as inverse dependence on the barrier height that parallels the dependence expressed in the Dexter and the superexchange formalism for EET in a D–B–A system. The distance dependence of singlet EET, SEET, in covalently linked D–B–A systems has been extensively studied.[4–12] Also the inverse dependence on the energy splitting has been studied, although far less comprehensively. However, to the best of our knowledge, no reports have appeared in the literature where the dependence of SEET on both these parameters have been studied in a single homogeneous series of D–B–A systems in which both have been varied systematically.

We have previously reported the synthesis and SEET studies of D–B–A systems (**ZnP-RB-H_2P**, see Figure 1) in which the donor–acceptor distances were kept the same, but the energy splitting between the donor and the bridge, i.e. the barrier height, was varied systematically. Now, we are interested in studying the distance, i.e. the barrier length, dependence in systems based on the same donor–acceptor couple and with the same relative donor–acceptor orientation to enable easy and productive comparison with our previous results. Therefore, we would like to extend our previous series by varying the bridge length with the prospect to explore the interplay between the effects of distance and energy splitting in a single series of homologous D–B–A systems (**ZnP-nB-H_2P**, see Figure 1).

This paper deals with the synthesis and characterization of this new subset of D–B–A systems and is organized as follows. First, the design of the porphyrin based D–B–A systems is discussed. Then the synthesis of these systems is presented. Finally, some important structural features of the bridge relevant to EET are discussed.

Results and Discussion

Design: In our continued efforts to understand the dependence of the exchange type of excitation energy transfer, EET, on the medium between the donor and the acceptor, a new subset of porphyrin dimers has been designed to allow for exploration of the impact of the energy barrier width on such transfer. The new subset of donor–bridge–acceptor, D–B–A, systems are composed of a zinc 15-aryl-2,3,7,8,12,13,17,18-octaalkylporphyrin as the donor (**ZnP**) and the corresponding free-base porphyrin as the acceptor (**H_2P**). The bridges (***n*B**) linking them together via the 5-positions are oligo(phenyleneethynylene)phenylenes (OPEs) of different lengths. The bridges vary from a total of two to five spacing phenylene units, **2B**, **3B**, **4B** and **5B**, respectively (Figure 1). As a general design principle for the new D–B–A systems, to allow for conclusive interpretations of the data from the photophysical measurements, the variations in all other parameters known to affect the EET process than these under scrutiny are kept to a minimum. Therefore, the D–B–A systems are constructed in such a way that (1) the relative donor–acceptor orientation is independent of the bridge, and (2) simple π-conjugation between the three components; donor, bridge, and acceptor, is minimized such as to preserve the spectroscopic identity of the three components in the system. However, it has not been possible to keep the energy splitting constant throughout the series of new systems. Therefore, in the systems reported in this paper, all parameters relevant to EET other

than the donor–acceptor length and the energy splitting are kept constant.

To meet these requirements the construction of the systems is based on the following: Firstly, because of the use of triple bonds in the bridge structure, the relative orientation between the donor and acceptor is the same in the different systems. Quantum mechanical calculations show that the angular distribution between the porphyrin planes and the central unit are almost uniform. The low rotational barrier calculated for rotation around a triple bond (<1 kcal/mol) in the bridge structures indicates that at room temperature all relative orientations of the porphyrin planes are energetically attainable and that fast interconversion between all possible conformations is to be expected.[14] Secondly, the π-conjugation between the components is minimized because of the steric effects imposed by the β-methyl groups closest to the bridge. This is shown by the conservation of the absorption spectra of the components in the assembly compared to the ones of the "free" components. Finally, the use of the phenyleneethynylene motif allows for a substantial variation in barrier width without affecting the relative donor–acceptor orientation. The donor–acceptor center-to-centre distances have been calculated to be 19.7, 26.5, 33.4, and 40.3 Å for the **2B**-, **3B**-, **4B**-, and **5B**-bridged dimers, respectively.[15,16]

Synthesis: The D–B–A systems were assembled from three intermediates or building blocks: (1) the donor building block in the form of an iodo functionalized zinc porphyrin, (2) the corresponding free-base porphyrin as the acceptor building block, and (3) an oligo(phenyleneethynylene)ethynyl compound as the bridge building block. To ensure the precise metallation state required to keep the photophysical measurements uncompromised, one porphyrin at a time was coupled to the bridge building block. To accomplish this sequential assembly without concomitant formation of troublesome symmetrical porphyrin dimers, the bridge building block had to be protected at one end in the first step of the D–B–A assembly.

Bridge building blocks: The bridge building blocks (TIPS-ethynyl-*n*B-ethynyl, see Scheme 1) used in the porphyrin dimer synthesis were prepared according to a literature procedure and the yields and NMR-data were in accordance with that reported.[17]

The synthesis commenced with a cross-coupling between 1,4-diiodobenzene and trimethylsilylethyne under normal Sonogashira reaction conditions yielding a statistical mixture of non-, mono- and disubstituted products. The monosubstituted 1-iodo-4-(trimethylsilylethynyl)benzene (**TMS-ethynyl-1B-I**) was then subjected to a second cross-coupling under the same conditions, albeit this time with the triisopropylsilyl (**TIPS**) protected alkyne. Subsequent deprotection with aqueous sodium hydroxide selectively removed the trimethylsilyl protective group affording the monoprotected diethynylbenzene (**TIPS-ethynyl-1B-ethynyl**). This is used as the bridge building block in the synthesis of the donor–bridge–acceptor, D–B–A, system with the second shortest bridge (**ZnP-3B-H_2P**). It is also the starting point for the synthesis of the bridge building blocks for the longer bridges. The bridge was elongated by one phenyleneethynylene unit in a two step sequence; the sequence starts with a standard Sonogashira cross-coupling to the product from the very first step (**TMS-ethynyl-1B-I**), followed by removal of the trimethylsilyl group by aqueous sodium hydroxide. This two-step reaction sequence is repeated until a bridge building block of the desired length is obtained. To obtain the terminated bridge building blocks (**ethynyl-*n*B**), the bridge building blocks of appropriate lengths were coupled to either iodobenzene or the monofunctionalized 1-iodo-4-phenylethynyl-benzene (**I-2B**)[18] following TMS removal, see Scheme 2. The terminated bridge building blocks except the longest one are either commercially available (**ethynyl-1B** = phenylacetylene) or obtained via literature procedures (**ethynyl-2B** and **ethynyl-3B**).[19] No reports on the isolation of **ethynyl-4B** could be found in the literature and its synthesis is therefore included in the experimental section. However, the deprotected **ethynyl-4B** proved to be very insoluble and unstable. Therefore, all characterization was performed on its TIPS-protected precursor (**TIPS-ethynyl-4B**) and all subsequent reactions including this compound were carried out immediately after deprotection.

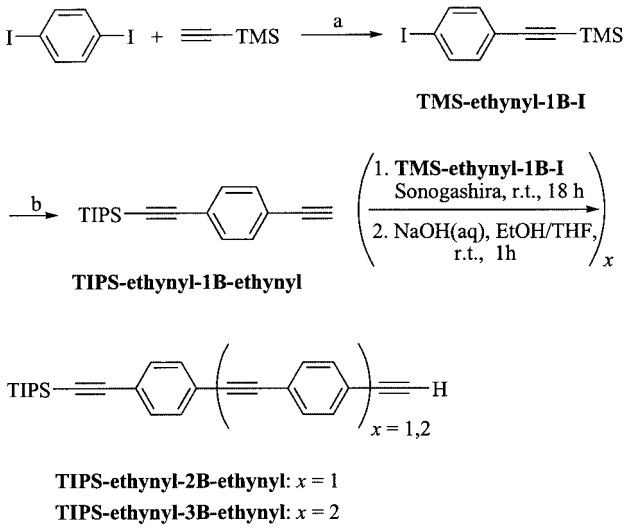

Scheme 1. (a) 2 mol-% $[Pd_2(dba)_3{\cdot}CHCl_3]$, 4 equiv. PPh_3 per Pd, 4 mol-% CuI, NEt_3, room temp., 1 h. (b) i. 1 equiv. of TIPS-acetylene, 2 mol-% $[Pd_2(dba)_3{\cdot}CHCl_3]$, 4 equiv. PPh_3 per Pd, 4 mol-% CuI, NEt_3, room temp., overnight; ii. 1 equiv. aqueous NaOH (1 M) in THF/EtOH, 1:1, room temp., 1 h.

The bridge reference compounds (***n*B**, see Figure 2) are either commercially available (**2B** = tolan) or available via literature procedures (**3B**[18] and **4B**[20]). Although described in the literature,[21] the product **5B** has been prepared using a different methodology and its synthesis is therefore included in the experimental section.

Porphyrin compounds: The larger structures comprising one or more porphyrin moieties were assembled using a modified Sonogashira coupling protocol to avoid metallation/transmetallation-problems associated with the copper presence.[22] Apart from this, the synthetic route was similar to that of the bridge building blocks with successive deprotections and couplings. The assembly of the series of D–B–

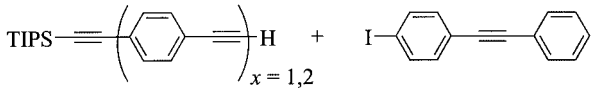

TIPS-ethynyl-1B-ethynyl: $x = 1$ **I-2B**
TIPS-ethynyl-2B-ethynyl: $x = 2$

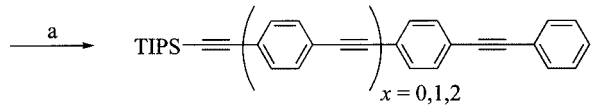

[*] **TIPS-ethynyl-2B:** $x = 0$
TIPS-ethynyl-3B: $x = 1$
TIPS-ethynyl-4B: $x = 2$

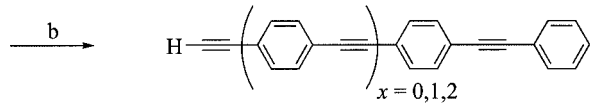

ethynyl-2B: $x = 0$
ethynyl-3B: $x = 1$
ethynyl-4B: $x = 2$

Scheme 2. (a) 2 mol-% $[Pd_2(dba)_3{\cdot}CHCl_3]$, 4 equiv. PPh_3 per Pd, 4 mol-% CuI, NEt_3, room temp., overnight. (b) 2 equiv. of TBAF in THF, room temp., 2 h. [*] Prepared using the same procedure but with iodobenzene instead of **I-2B**.

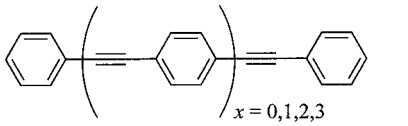

2B: $x = 0$ **3B**: $x = 1$ **4B**: $x = 2$ **5B**: $x = 3$

Figure 2. The bridge reference chromophores ***n*B**.

A systems, **ZnP-*n*B-H_2P**, began with a palladium-catalyzed cross-coupling between the arylic iodide moiety of the porphyrin building block and the terminal alkyne of one of the mono protected bridge building blocks (see Scheme 3).

The conditions used for this coupling were the ones developed by Wagner et al.[23] featuring a high loading of triphenylarsane and $[Pd_2(dba)_3{\cdot}CHCl_3]$ together with triethylamine as base and in the absence of cuprous iodide. The triisopropylsilyl protected alkyne was then deprotected using fluoride ions followed by a final cross-coupling performed under the same conditions as the previous one. The first porphyrin coupled to a bridge building block was in all cases but one pre-metallated with zinc. Consequently the last porphyrin units coupled to complete the diporphyrins were in all cases but one a free-base porphyrin. The reversed order of coupling for one of the systems was based on solu-

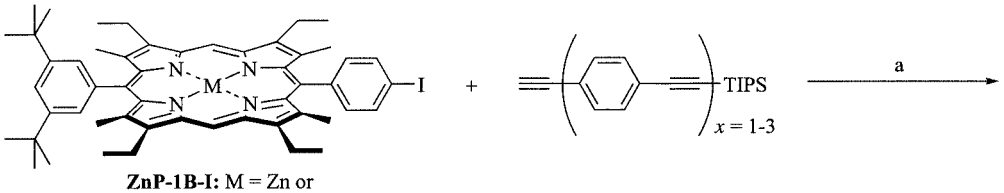

ZnP-1B-I: M = Zn or
H_2P-1B-I: M = 2H

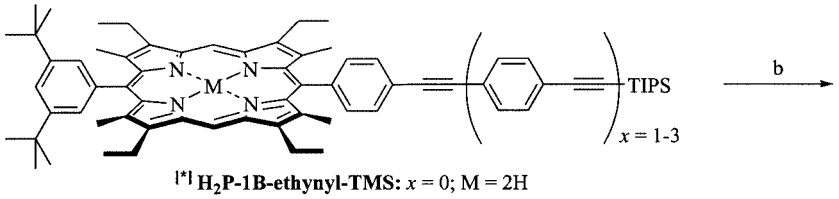

[*] **H_2P-1B-ethynyl-TMS:** $x = 0$; M = 2H
ZnP-2B-ethynyl-TIPS: $x = 1$; M = Zn
ZnP-3B-ethynyl-TIPS: $x = 2$; M = Zn
H_2P-4B-ethynyl-TIPS: $x = 3$; M = 2H

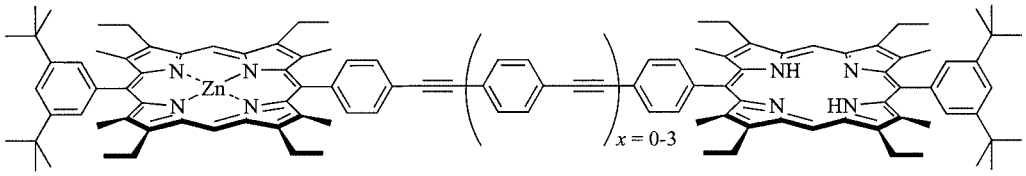

ZnP-2B-H_2P: $x = 0$
ZnP-3B-H_2P: $x = 1$
ZnP-4B-H_2P: $x = 2$
ZnP-5B-H_2P: $x = 3$

Scheme 3. (a) 15% $[Pd_2(dba)_3{\cdot}CHCl_3]$, 4 equiv. $AsPh_3$ per Pd, toluene/NEt_3, 3:1, 40 °C, 5–18 h (b) i. TBAF, THF, room temp., 30 min; ii. 15% $[Pd_2(dba)_3{\cdot}CHCl_3]$, $AsPh_3$ 4 equiv. per Pd, **ZnP-1B-I** or **H_2P-1B-I**, toluene/NEt_3, 3:1, 40 °C, 5–18 h, [*] **H_2P-1B-ethynyl-TMS** was produced by direct condensation of a TMS-protected *p*-ethynyl-substituted benzaldehyde in the porphyrin ring synthesis. Therefore only step (b) in the Scheme is applicable to the synthesis of **ZnP-2B-H_2P**.

bility and purification considerations. The zinc/free-base dimers were by this approach produced directly in a precise state of metallation. The shortest dimer, **ZnP-2B-H_2P** (x = 0, Scheme 3), was prepared from the cross-coupling of the functionalized porphyrin building blocks **ZnP-1B-I** and **H_2P-1B-ethynyl** using the same modified Sonogashira protocol. All of the porphyrin building blocks together with the dimer **ZnP-3B-H_2P** were available from our previous work on donor–bridge–acceptor systems.[18] The reference compound **ZnP-3B** with x = 1 shown in Scheme 4 was also available from this work. The other reference compounds, **ZnP-*n*B**, were assembled using the same modified Sonogashira protocol as the dimers, the only difference being the use of truncated bridge building blocks (**ethynyl-*n*B**) instead of difunctionalized ones (see Scheme 4). The coupling was performed using a pre-metallated iodo-functionalized porphyrin in all cases but one. For the shortest bridge, x = 0, metallation of the porphyrin was performed in the last step due to purification advantages. Regardless of in which order the synthesis was performed, the zinc insertion produced excellent yields.

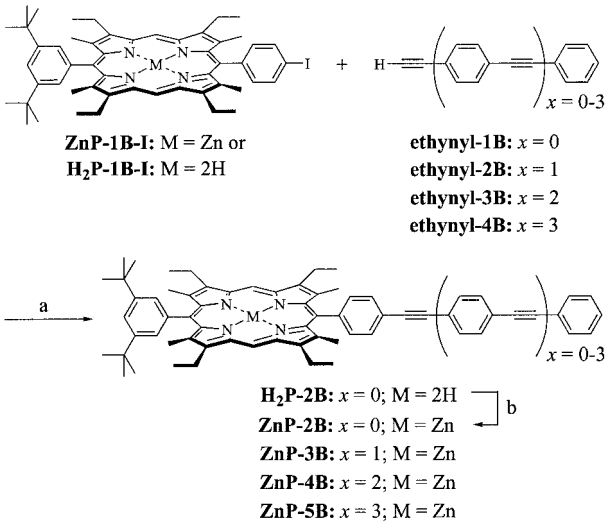

Scheme 4. (a) 15% [$Pd_2(dba)_3$·$CHCl_3$], 4 equiv. $AsPh_3$ per Pd, toluene/NEt_3, 3:1, 40 °C, 5–18 h. (b) $Zn(OAc)_2$·$2H_2O$/MeOH, $CHCl_3$, room temp., 2 h.

Characterization: The ^{1}H and ^{13}C NMR spectroscopic data were in accordance with what would be expected. Furthermore, HRMS confirmed that the desired products were obtained. Spectra from ^{13}C NMR and FAB$^+$ HRMS are provided in the Supporting Information. The purity of the products obtained via the present protocol were very good as judged from NMR spectroscopy. This was also confirmed by more sensitive methods, i.e. steady-state and time-resolved spectroscopy. Both methods were employed to characterize the systems further and to reveal their EET properties. The photophysical studies in combination with quantum chemical studies, and a thorough discussions on the interplay between the effects of length and the energy difference between the donor and the bridge, ΔE_{DB}, on the superexchange mechanism for energy transfer is given elsewhere.[24] The high purity is most clearly indicated by that the decay of the singlet excited state of the ZnP donor could be fitted to a single exponential decay for all of the newly prepared systems except one. The short lifetime of **ZnP-2B-H_2P** makes the studies of this much more sensitive to trace amounts of impurities and a second exponential decay with a minute preexponential factor was used to fit the data from this. A building block approach was used to ensure the integrity of the metallation states. The presence of two distinct signals corresponding to the meso protons in the ^{1}H NMR spectrum in all cases and the overall nice fit to a single exponential decay confirmed this. Furthermore, the ground state absorption spectra of the different porphyrinic compounds were identical to the sum of the three components, the donor **ZnP**, the bridge ***n*B**, and the acceptor H_2P. This also indicates that the design was successful in preventing π-conjugation between the bridge and the donor or acceptor.

The difference between the previous system **ZnP-RB-H_2P** and the topical system **ZnP-*n*B-H_2P** lies in the nature of the bridges. The energy splitting between the lowest excited states of the donor and the bridge, ΔE_{DB}, is of crucial importance in determining the operating mechanisms for EET (hopping vs. direct). Furthermore, we have previously shown the bridge mediated EET rate to correlate to the inverse quadratic energy splitting (ΔE_{DB}^{-2}) in the **ZnP-RB-H_2P** series.[14,25] All of the new bridges have higher lying first excited states than the donor. If the energies for the $S_0 \rightarrow S_1$ transitions in the topical bridges are taken as the midpoint between the corresponding absorption and emission bands, as indicated in Figure 3, then ΔE_{DB} for **2B**, **3B**, **4B**, and **5B** is 15 800, 11 600, 9 700, and 8 800 cm^{-1}, respectively. The differences in energies are all large enough to prevent a hopping mechanism for the energy transfer, and superexchange is the only bridge dependent mechanism to be expected. Thus, these systems are well suited for studying bridge mediation effects, but the variation in ΔE_{DB} accompanying the variation in length has to be considered when evaluating the data.

To reveal the bridge mediating effects, the shares of EET accounted for by bridge dependent through-bond and bridge independent through-space mechanisms have to be established. Singlet–singlet EET can be efficiently transferred through-space over long distances without the aid of any bridge via a Coulombic dipole–dipole interaction, i.e. the via the Förster mechanism. A higher EET rate than what would be expected from the calculated Förster rate could in these systems be attributed to a "mediation effect" of the bridges, i.e. to a superexchange/through-bond mechanism. To calculate the rate constant for the bridge mediated EET, k_{med}, the rate constant, $k_{För}$, for EET according to Förster [Equation (1)] is subtracted from the experimental rate constant k for EET, calculated from the measured lifetimes of the excited donor.

$$k_{För} = \frac{9000 \ln 10}{128\pi^5 N_A} \frac{\Phi_D \kappa^2 J}{\tau_D R_{cc}^6 n^4} \quad (1)$$

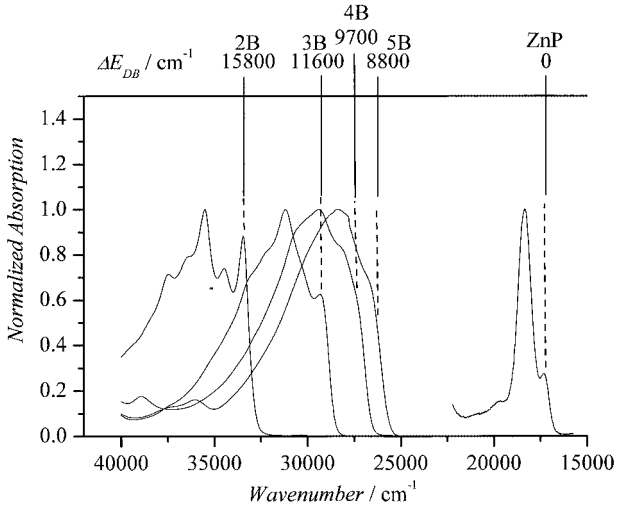

Figure 3. Normalized absorption spectra for the four bridge molecules and the **ZnP** donor in toluene. The energy difference, ΔE_{DB}, between the $S_0 \rightarrow S_1$ transition for the donor and the bridges are indicated by vertical bars.

The quantum yield, Φ_D, and the lifetime, τ_D, of the donor are both defined in absence of the acceptor. N_A is Avogadros number, n the refractive index of the solvent and R_{cc} the centre-to-centre distance between donor and acceptor. The orientation factor, κ^2, describes the relative orientation of the donor and acceptor transition moments, i.e. the two interacting dipoles. It has been shown that κ^2 varies between 2/3 and 1 for the different configurations of the porphyrin planes of this particular donor–acceptor system. Therefore, the dynamic average of 5/6 is used for κ^2 in the calculations. Further, J is the Förster spectral overlap integral defined as [Equation (2)].

$$J = \frac{\int_0^\infty F_D(\lambda)\varepsilon_A(\lambda)\lambda^4 d\lambda}{\int_0^\infty F_D(\lambda)d\lambda} \quad (2)$$

where $F_D(\lambda)$ is the fully corrected fluorescence intensity of the donor, and $\varepsilon_A(\lambda)$ is the acceptor molar absorptivity.

In distance dependence studies where the bridge is expected to mediate the exchange interaction, i.e. via superexchange,[3] it is customary to evaluate the bridge efficiency as a mediator or conduit by calculating its resistance or attenuation factor. The electronic coupling for superexchange is assumed to approximately decay exponentially with distance, thus the rate constant is generally described by the following expression [Equation (3)].

$$k_{ex} = A \exp(-\beta R_{cc}) \quad (3)$$

where β is the attenuation factor. The donor–acceptor distance used in this approximation is usually the edge-to-edge distance, R_{ee}. However the difference in magnitude between the β values obtained by fitting a linear function to the plot of the natural logarithm of the transfer rates vs. either R_{cc} or R_{ee} is small for these systems. Therefore, in the subsequent discussion only the centre-to-centre distances will be used to avoid the discussion to become unnecessarily complex.

The donor–acceptor distance is a crucial factor in determining the rate of EET transfer by either the through-space or the through-bond mechanisms. In this new subset of molecules studied, viz. **ZnP-2B-H$_2$P**, **ZnP-3B-H$_2$P**, **ZnP-4B-H$_2$P**, and **ZnP-5B-H$_2$P** (Figure 1), the DFT-calculated centre-to-centre distances vary from 19 to 40 Å.[24] These values give good estimations of the donor-acceptor distances, but their validity in calculations using the Förster theory depend on the rigidity of the OPE structural elements. Oligo(phenyleneethynylene) is often considered as a rigid structure and we have also chosen to treat it as such. However, NMR-studies reported in the literature suggest a relatively high flexibility in these kinds of structures.[26] Because the donor–acceptor centre-to-centre distance R_{cc} is one of the dominating parameters governing EET via the Förster mechanism, it thus seems appropriate to discuss the potential variation in R_{cc} due to conformational changes and its effect on the EET. There are several ways to estimate the dynamic average donor–acceptor distances. NMR-studies[26] have been used and extensive computational modelling could be an alternative. However, it is also possible to use the data that we have from our previous studies on the **ZnP-RB-H$_2$P** system (see Figure 1) if a few simplifications are made. Furthermore, because one of the members of the **ZnP-*n*B-H$_2$P** series, **ZnP-2B-H$_2$P**, is very similar to the diporphyrin used in the NMR-study performed by Bothner-By et al.,[26] a comparison to check how well the estimates from the different approaches match is possible. Our estimates are derived from a small discrepancy between the experimentally determined SEET rate constant for the **ZnP-OB-H$_2$P** system (see Figure 1) and the one calculated using the Förster approximation (vide supra).[14] For a full description of the model used to obtain dynamic average donor–acceptor distances for the members of the **ZnP-*n*B-H$_2$P** series, see Supporting Information.

The through-bond electronic coupling for the **ZnP-OB-H$_2$P** system is so small that it does not result in any detectable triplet EET.[27] Because triplet EET is governed by orbital overlap dependent mechanisms, this result indicates that the only available SEET mechanism for this system is the Förster mechanism. Consequently, any rate enhancement compared to the rate constant calculated according to the Förster theory could be assumed to be an effect of conformational dynamics. From these data, we can calculate the dynamic average donor–acceptor distance for the **ZnP-OB-H$_2$P** system if the following three assumptions are made: (1) The discrepancy between the experimental and the calculated rate constants is not caused by the use of any erroneous numerical values of the parameters in the calculation of the Förster rate constant. (2) There are no changes in numerical values of these parameters, other than in the donor–acceptor distance, due to the structural dy-

namics. (3) The through-bond coupling is negligible. In other words, the EET rate enhancement is due exclusively to a reduction of the donor–acceptor distance. The third assumption is supported by several structural features of the **OB**-bridge disfavoring its efficacy as conduit for electronic coupling; the *s-cis* conformation into which the bicyclooctane moiety is looked,[13] the clear separation of the coupling pathway into two π-systems separated by a σ-skeleton,[28] and its high singlet excitation energy compared to that of the donor.[14] The absence of triplet EET in the **ZnP-OB-H_2P** system clearly reflects this insulating property.[27]

The dynamic average donor–acceptor distance can then be obtained as the product of the donor–acceptor distance in the extended **ZnP-OB-H_2P** system and the sixth root of the quotient between the calculated Förster rate constant for the extended conformation and the experimentally determined one. The donor-acceptor distance for the fully extended and energy-optimized conformation of the **ZnP-OB-H_2P** system is found to be 26.4 Å (DFT B3LYP/6-31G*), the EET rate constant in CH_2Cl_2 was calculated to $2.6 \cdot 10^8$ s^{-1}, and experimentally found to be $3.7 \cdot 10^8$ s^{-1}.[14] The dynamic average donor-acceptor distance is then calculated to 24.8 Å.

This reasoning can be extrapolated to cover the ***n*B**-bridged systems if we assume the overall bending force constants for the **OB** and the **3B** bridges to be identical. Further, if the bridges are pictured as rods consisting of a series of identical structural elements all characterized by the same bending force constant, then the overall bending force constant is equal to the bending force constants for the constituent structural elements divided by the number of elements. The number of structural elements is arbitrarily chosen as the number of atoms of the bridges, including the *meso* carbons that lie on the line connecting the porphyrin centres, i.e. the contribution from the aromatic rings and bicyclooctane is neglected. And finally, the available energy for bending motion is, at a given temperature, the same for all systems. According to this model, the reduction in donor–acceptor distances increases with increasing bridge length. The reduction in donor–acceptor distances are between 4–9% of the centre-to-centre distances estimated from the geometry optimized structures. There are large uncertainties in the calculated dynamic average donor–acceptor distances, because of the minute difference between the experimental and the calculated transfer rate upon which the model is based. However, it is worth noting that through this simplistic treatment of the structural dynamics we obtain a dynamic average bending of 28° for the **ZnP-2B-H_2P** system, in very good agreement with the 26° found by the elegant NMR studies reported by Bothner-By et al.[26]

For all members of the **ZnP-*n*B-H_2P** series, the rate constant for mediation, k_{med} – the difference between the k and $k_{För}$ – explains more than 60% of the donor fluorescence quenching when the DFT-calculated centre-to-centre distances are used (Supporting Information, Table S2).[24] Such a rate enhancement caused by a superexchange-mediated through-bond contribution is in line with our previous observations, because of the smaller energy differences, ΔE_{DB}, between the new bridges and the donor, compared to that of the previously mentioned **OB**-bridge (17600 cm^{-1}). This observation is also supported by the work of Lindsey et al. who have reported that EET is the major deactivation pathway for systems similar to **ZnP-2B-H_2P**, with an even larger mediation contribution.[29]

When the somewhat shorter dynamic average donor–acceptor distances are used in recalculations of the through-space transfer rates and mediation contributions, a constant mediation contribution of ca. 53% is observed for the two shortest systems, whereas a drop in the mediation contribution to 41% and 26% is seen for **ZnP-4B-H_2P** and **ZnP-5B-H_2P**, respectively (Supporting Information, Table S2). This is an effect of the larger Förster rate constant caused by the reduction in through-space donor–acceptor distance. However, it is important to note that the through-bond length is not affected, or only marginally so, by conformational bending, only the through-space distance is affected.

When the DFT-calculated centre-to-centre distances are used an attenuation factor $\beta = 0.20$ $Å^{-1}$ is obtained.[24] If the estimated dynamic average donor–acceptor distances are used instead the attenuation factor becomes $\beta = 0.28$ $Å^{-1}$ with an excellent fit. Although the attenuation factor β is system specific and depends on system parameters such as ΔE_{DB}, it has often been regarded as a measure of how efficient a specific class of bridge act as conduit. A comparison could therefore be informative and give at least some qualitative measure of how efficient mediator the bridge type is compared to others. Attenuation factors for EET along different conjugated bridges have been reported by other groups; $\beta = 0.32$ $Å^{-1}$ and $\beta = 0.33$ $Å^{-1}$ for oligo(phenylene) bridges,[9,10] $\beta = 0.17$ for alkyne bridges,[11] and $\beta = 0.11$ $Å^{-1}$ for dialkoxy-substituted oligo(*p*-phenyleneethynylene) bridges.[12] The obtained β value for SEET via oligo(phenyleneethynylene) thus indicates that this bridge type is a better conduit in this context than oligo(phenylene) and less efficient than oligo(ethynylene) or its dialkoxy-substituted counterpart. The β-values of the OPE motif fits in at the same position in this general pattern either if the DFT-calculated distances or the dynamic average estimates are used.

Despite a proven significant mediation contribution, a slope of –5.9 was obtained by linear fitting to the plot of $\ln k$ vs. $\ln R_{cc}$ when the DFT-calculated donor–acceptor distances were used.[24] When the recalculated values using the dynamic average donor–acceptor distances are used, a slope of –6.5 is obtained. Regardless of the distance used, the value is close to –6.0, the theoretical value for dipole–dipole coupling as described by the Förster equation, often used as an indicator for through-space transfer. It is also worth noting that if the DFT-calculated centre-to-centre distances are used in the evaluations, the share of through-space transfer is smaller, but the slope is closer to the theoretical value for dipole–dipole coupling as described by the Förster equation. This shows that fitting $\ln k$ vs. $\ln R$ and taking the slope of –6 as a proof for the Förster mechanism can be misleading.

Conclusions

A series of zinc/free-base porphyrin dimers have been synthesized for the purpose of excitation energy transfer, EET, studies. A building block approach using palladium-catalyzed alkynylations gave the diporphyrins of high purity in a precise state of metallation and in good yields. The donor–bridge–acceptor, D–B–A, systems were designed to enable delineation of the impact of critical geometric and electronic parameters on the EET transfer rate. The OPE structural element of the bridge allowed a stepwise increase in length, with a limited decrease in energy of the first excited singlet state, thus allowing studies of a mediating effect in the absence of a hopping mechanism. This structural element was shown to be somewhat flexible, but stiff enough to give comparable results when the evaluations were made using dynamic average or DFT-calculated donor–acceptor distances. Estimates of the dynamic average donor–acceptor distances were obtained from a simple mechanical model of the bridge, where the bending force constant was derived from a difference in a calculated and observed EET transfer rate.

Experimental Section

Materials: Diethyl ether, toluene and tetrahydrofuran (THF) were dried by distillation from sodium/benzophenone under nitrogen. Dichloromethane and triethylamine were dried by distillation from calcium hydride under nitrogen. Dried solvents were used immediately following distillation. Other commercially available reagents were purchased from Aldrich or Lancaster and used without further purification.

Methods: Deaeration of reaction mixtures was achieved by bubbling argon through the solution for 30 minutes. Palladium-catalyzed reactions were performed under argon and protected from light by aluminium foil. Column chromatography and flash chromatography was generally performed using silica gel (Matrex, LC 60 Å/35–70 micron). Chromatography of porphyrins was performed using silica gel (Merck, grade 60, 230–400 mesh). Size exclusion chromatography (SEC) was performed on BioRad Bio-Beads SX–3 in toluene. ^{1}H (400 MHz) and ^{13}C (100.6 MHz) NMR spectra were recorded at room temp. in $CDCl_3$, [D_5]chlorobenzene or [D_2]tetrachloroethane, using a Jeol Eclipse 400 NMR spectrometer and a Varian UNITY 400 NMR spectrometer. Chemical shifts are reported relative to tetramethylsilane (δ_H = 0 ppm) and all coupling constants given are for (H,H) couplings. Positive FAB high resolution mass spectra were obtained on a JEOL SX102 mass spectrometer at Instrumentstationen, Lund University, Sweden. Samples were desorbed from a 3-NBA matrix using 6 kV xenon atoms. Elemental analyses were performed by H. Kolbe Mikroanalytisches Laboratorium, Mülheim an der Ruhr, Germany.

TIPS-ethynyl-4B: [$Pd_2(dba)_3$·$CHCl_3$] (4 mg, 4 μmol) was added to a deaerated solution of **ethynyl-2B-ethynyl-TIPS** (77 mg, 0.200 mmol), **I-2B** (61 mg, 0.200 mmol), PPh_3 (8 mg, 32 μmol) and CuI (1.5 mg, 8 μmol) in NEt_3 (15 mL). The reaction mixture was stirred overnight, filtered and concentrated. Flash chromatography (SiO_2, pentane followed by CH_2Cl_2) and recrystallization from EtOAc yielded the desired product, **TIPS-ethynyl-4B**, as a white solid (77 mg, 0.138 mmol, 69%); ^{1}H NMR ($CDCl_3$): δ = 1.13 (m, 21 H, *i*Pr), 7.36 (m, 3 H, ArH), 7.46 (m, 4 H, ArH), 7.52 (m, 8 H, ArH), 7.54 (m, 2 H, ArH) ppm; elemental analysis calcd. (%) for $C_{41}H_{38}Si$ (558.8); C 88.12 H 6.85; found: C 87.94, H 6.81.

Ethynyl-4B: A sample of **TIPS-ethynyl-4B** (73 mg, 130 μmol) was dissolved in THF (5 mL). Bu_4NF (260 μmol, 260 μL of a 1.0 M solution in THF) was added and the mixture was stirred at room temp. for 2 h. The product **ethynyl-4B** is highly insoluble in almost all organic media and precipitates rapidly. The white solid was separated by means of centrifugation and was used directly in the synthesis of **ZnP-5B** without further purification and characterization due to its instability and exceedingly poor solubility.

5B: [$Pd_2(dba)_3$·$CHCl_3$] (5 mg, 5 μmol) was added to a deaerated solution of **ethynyl-3B** (79 mg, 0.261 mmol), **I-2B** (79 mg, 0.261 mmol), PPh_3 (10 mg, 40 μmol) and CuI (1.9 mg, 10 μmol) in toluene/NEt_3, 1:1 (10 mL). The reaction mixture was stirred overnight at room temp. The solvent was evaporated and the residue triturated with methanol to remove unwanted material. The remaining residue was triturated with PhCl using a soxhlet apparatus. The pure product **5B** crystallized directly from the solution upon cooling to room temperature affording a white crystalline solid (50 mg, 0.104 mmol, 40%); elemental analysis calcd. (%) for $C_{38}H_{22}$ (478.6); C 95.37 H 4.63; found: C 95.23, H 4.58

ZnP-2B-H2P: [$Pd_2(dba)_3$·$CHCl_3$] (6 mg, 6 μmol) was added to a deaerated solution of **H_2P-1B-ethynyl** (35 mg, 0.046 mmol), **ZnP-1B-I** (42 mg, 0.045 mmol) and $AsPh_3$ (15 mg, 48 μmol) in dry toluene/NEt_3 (3:1, 12 mL). The reaction mixture was stirred overnight at 40 °C and the solvent was removed in vacuo. Chromatography (silica gel, CH_2Cl_2 followed by 2% MeOH in CH_2Cl_2) and SEC gave **ZnP-2B-H_2P** as a red solid (39 mg, 0.025 mmol, 56%); ^{1}H NMR ($CDCl_3$): δ = –2.39 ppm (br. s, 2 H, NH), 1.52 (s, 18 H, *t*Bu), 1.53 (s, 18 H, *t*Bu), 1.81 (m, 24 H, -CH_2CH_3), 2.46 (s, 6 H, pyrrole-CH_3), 2.48 (s, 6 H, pyrrole-CH_3), 2.63 (s, 6 H, pyrrole-CH_3), 2.65 (s, 6 H, pyrrole-CH_3), 4.06 (m, 16 H, -CH_2CH_3), 7.83 (m, 2 H, ArH), 7.93 (d, ^4J = 2 Hz, 2 H, ArH), 7.95 (d, ^4J = 2 Hz, 2 H, ArH), 8.13 (m, 4 H, ArH), 8.21 (m, 4 H, ArH), 10.25 (s, 2 H, *meso*), 10.28 (s, 2 H, *meso*) ppm. HRMS (FAB) calcd. for $[C_{106}H_{120}N_8Zn]^+$: 1568.8927, found: 1568.8944.

ZnP-3B-ethynyl-TIPS: $Pd_2(dba)_3$·$CHCl_3$ (8 mg, 8 μmol) was added to a deaerated solution of **ZnP-1B-I** (50 mg, 0.054 mmol), **TIPS-ethynyl-2B-ethynyl** (31 mg, 0.081 mmol), $AsPh_3$ (20 mg, 65 μmol) and toluene/NEt_3 (16 mL, 3:1). The reaction mixture was stirred for 5 h at 40 °C and the solvent removed in vacuo. Chromatography on silica (pentane/diethyl ether, 10:1) followed by SEC gave **ZnP-3B-ethynyl-TIPS** as a red solid (40 mg, 0.034 mmol, 63%); ^{1}H NMR ($CDCl_3$): δ = 1.15 [m, 21 H, Si(*i*Pr)], 1.52 (s, 18 H, *t*Bu), 1.77 (m, 12 H, -CH_2CH_3), 2.45 (s, 6 H, pyrrole-CH_3), 2.51 (s, 6 H, pyrrole-CH_3), 4.01 (m, 8 H, -CH_2CH_3), 7.50 (m, 4 H, ArH), 7.60 (d, ^3J = 8 Hz, 2 H, ArH), 7.69 (d, ^3J = 8 Hz, 2 H, ArH), 7.82 (t, ^4J = 2 Hz, 1 H, ArH), 7.94 (m, 4 H, ArH), 8.10 (d, ^3J = 8 Hz, 2 H, ArH), 10.18 (s, 2 H, *meso*) ppm. HRMS (FAB) calcd. for $[C_{79}H_{88}N_4SiZn]^+$: 1184.6070, found: 1184.6067.

ZnP-3B-ethynyl: A sample of **ZnP-3B-ethynyl-TIPS** (23 mg, 0.021 mmol) was dissolved in THF (3 mL). Bu_4NF (25 μmol, 25 μL of a 1.0 M solution in THF) was added and the mixture was stirred at room temp. for 30 minutes during which the colour turned darker red. Methanol was added to precipitate the porphyrin and subsequent centrifugation gave **ZnP-3B-ethynyl** as a red solid (17 mg, 0.018 mmol, 86%); The product was used directly in the synthesis of **ZnP-4B-H_2P** without other characterization than FAB-MS and ^{1}H NMR due to its instability; ^{1}H NMR ($CDCl_3$): δ = 1.52 (s, 18 H, *t*Bu), 1.80 (m, 12 H, -CH_2CH_3), 2.47 (s, 6 H, pyrrole-CH_3), 2.54 (s, 6 H, pyrrole-CH_3), 3.21 (s, 1 H, alkyne-H), 4.03 (m, 8 H, -CH_2CH_3), 7.53 (m, 4 H, ArH), 7.62 (d, ^3J = 8 Hz,

2 H, ArH), 7.71 (d, ^3J = 8 Hz, 2 H, ArH), 7.84 (t, ^4J = 2 Hz, 1 H, ArH), 7.96 (m, 4 H, ArH), 8.13 (d, ^3J = 8 Hz, 2 H, ArH), 10.21 (s, 2 H, *meso*) ppm. HRMS (FAB) calcd. for $[C_{70}H_{68}N_4Zn]^+$: 1028.4735, found: 1028.4734.

ZnP-4B-H2P: Prepared from **H_2P-1B-I** (36 mg, 0.042 mmol) and **ZnP-3B-ethynyl** (33 mg, 0.032 mmol) as described for **ZnP-2B-H_2P** and gave **ZnP-4B-H_2P** as a red solid (19 mg, 0.011 mmol, 34%); ^{1}H NMR ($CDCl_3$): δ = –2.43 ppm (br. s, 2 H, NH), 1.51 (s, 18 H, *t*Bu), 1.52 (s, 18 H, *t*Bu), 1.79 (m, 24 H, -CH_2CH_3), 2.45 (s, 6 H, pyrrole-CH_3), 2.47 (s, 6 H, pyrrole-CH_3), 2.55 (s, 6 H, pyrrole-CH_3), 2.57 (s, 6 H, pyrrole-CH_3), 4.03 (m, 16 H, -CH_2CH$_3$), 7.67 (m, 4 H, ArH), 7.74 (m, 4 H, ArH), 7.82 (m, 2 H, ArH), 7.92 (d, ^4J = 2 Hz, 2 H, ArH), 7.94 (d, ^4J = 2 Hz, 2 H, ArH), 7.97 (m, 4 H, ArH), 8.13 (m, 4 H, ArH), 10.22 (s, 2 H, *meso*), 10.25 (s, 2 H, *meso*) ppm. HRMS (FAB) calcd. for $[C_{122}H_{128}N_8Zn]^+$: 1768.9553, found: 1768.4747.

H_2P-4B-ethynyl-TIPS: Prepared from **H_2P-1B-I** (100 mg, 0.116 mmol) and **TIPS-ethynyl-3B-ethynyl** (69 mg, 0.144 mmol) as described for **ZnP-2B-H_2P** and gave **H_2P-4B-ethynyl-TIPS** as a red solid (99 mg, 0.081 mmol, 70%); ^{1}H NMR ($CDCl_3$): δ = –2.41 ppm (br. s, 2 H, NH), 1.14 (m, 21 H, Si(*i*Pr)), 1.51 (s, 18 H, *t*Bu), 1.78 (m, 12 H, -CH_2CH_3), 2.46 (s, 6 H, pyrrole-CH_3), 2.56 (s, 6 H, pyrrole-CH_3), 4.03 (m, 8 H, -CH_2CH$_3$), 7.48 (m, 4 H, ArH), 7.54 (m, 4 H, ArH), 7.61 (d, ^3J = 8 Hz, 2 H, ArH), 7.69 (d, ^3J = 8 Hz, 2 H, ArH), 7.81 (t, ^4J = 2 Hz, 1 H, ArH), 7.92 (d, ^4J = 2 Hz, 2 H, ArH), 7.94 (d, ^3J = 8 Hz, 2 H, ArH), 8.11 (d, ^3J = 8 Hz, 2 H, ArH), 10.24 (s, 2 H, *meso*) ppm. HRMS (FAB) calcd. for $[C_{87}H_{94}N_4SiZn]^+$: 1222.7248, found: 1222.7242.

H_2P-4B-ethynyl: Prepared by TIPS deprotection of **H_2P-4B-ethynyl-TIPS** (96 mg, 0.078 mmol) as described for **ZnP-3B-ethynyl** and gave **H_2P-4B-ethynyl** as a red solid (83 mg, 0.078 mmol, 100%). The product was used directly in the synthesis of **ZnP-5B-H_2P** without further purification or other characterization than FAB-MS due to its instability and exceedingly poor solubility in all organic solvents. HRMS (FAB) calcd. for $[C_{78}H_{74}N_4]^+$: 1066.5913, found: 1066.5923.

ZnP-5B-H_2P: Prepared from **ZnP-1B-I** (79 mg, 0.085 mmol) and **H_2P-4B-ethynyl** (83 mg, 0.078 mmol) as described for **ZnP-2B-H_2P** and gave **ZnP-5B-H_2P** as a red solid (61 mg, 0.033 mmol, 45%); ^{1}H NMR ([D$_5$]chlorobenzene): δ = –1.84 ppm (br. s, 1 H, NH), –1.79 (br. s, 1 H, NH), 1.49 (s, 18 H, *t*Bu), 1.51 (s, 18 H, *t*Bu), 1.81 (m, 24 H, -CH_2CH_3), 2.63 (m, 12 H, pyrrole-CH_3), 2.64 (s, 6 H, pyrrole-CH_3), 2.65 (s, 6 H, pyrrole-CH_3), 4.04 (m, 16 H, -CH_2CH$_3$), 7.50–7.66 (m, 12 H, ArH), 7.94 (m, 10 H, ArH), 8.05 (m, 4 H, ArH), 10.36 (s, 2 H, *meso*), 10.42 (s, 2 H, *meso*) ppm. HRMS (FAB) calcd. for $[C_{130}H_{132}N_8Zn]^+$: 1868.9866, found: 1868.9881.

H_2P-2B: Prepared from **H_2P-1B-I** (50 mg, 0.058 mmol) and phenylacetylene (59 mg, 0.580 mmol) as described for **ZnP-2B-H_2P** and gave **H_2P-2B** as a red solid (37 mg, 0.044 mmol, 76%); ^{1}H NMR ($CDCl_3$): δ = –2.43 ppm (br. s, 2 H, NH), 1.51 (s, 18 H, *t*Bu), 1.78 (m, 12 H, -CH_2CH_3), 2.46 (s, 6 H, pyrrole-CH_3), 2.56 (s, 6 H, pyrrole-CH_3), 4.03 (m, 8 H, -CH_2CH$_3$), 7.45 (m, 3 H, ArH), 7.71 (m, 2 H, ArH), 7.81 (t, ^4J = 2 Hz, 1 H, ArH), 7.91 (d, ^4J = 2 Hz, 2 H, ArH), 7.94 (d, ^3J = 8 Hz, 2 H, ArH), 8.10 (d, ^3J = 8 Hz, 2 H, ArH), 10.24 (s, 2 H, *meso*) ppm. HRMS (FAB) calcd. for $[C_{60}H_{66}N_4]^+$: 842.5287; found: 842.5270.

ZnP-2B: The free-base porphyrin **H_2P-2B** (13 mg, 0.015 mmol) was dissolved in 10 mL $CHCl_3$ and $Zn(OAc)_2{\cdot}2H_2O$ (10 mg, 0.045 mmol) dissolved in MeOH (1 mL) was added. The reaction was stirred at room temperature for 2 h. The reaction mixture was washed twice with 10% $NaHCO_3$ and twice with water. Evaporation of the solvent gave **ZnP-2B** as a red solid (14 mg, 0.015 mmol, 100%); ^{1}H NMR ($CDCl_3$): δ = 1.51 (s, 18 H, *t*Bu), 1.77 (m, 12 H, -CH_2CH_3), 2.44 (s, 6 H, pyrrole-CH_3), 2.53 (s, 6 H, pyrrole-CH_3), 4.01 (m, 8 H, -CH_2CH$_3$), 7.44 (m, 3 H, ArH), 7.72 (dd, ^3J = 8 Hz, ^4J = 2 Hz, 2 H, ArH), 7.82 (t, ^4J = 2 Hz, 1 H, ArH), 7.94 (m, 4 H, ArH), 8.10 (d, ^3J = 8 Hz, 2 H, ArH), 10.19 (s, 2 H, *meso*) ppm. HRMS (FAB) calcd. for $[C_{60}H_{64}N_4Zn]^+$: 904.4422; found: 904.4428.

ZnP-4B: Prepared from **ZnP-1B-I** (20 mg, 0.022 mmol) and **ethynyl-3B** (9 mg, 0.030 mmol) as described for **ZnP-3B-ethynyl-TIPS** and gave **ZnP-4B** as a red solid (8 mg, 0.007 mmol, 34%); ^{1}H NMR ($CDCl_3$): δ = 1.51 (s, 18 H, *t*Bu), 1.78 (m, 12 H, -CH_2CH_3), 2.44 (s, 6 H, pyrrole-CH_3), 2.53 (s, 6 H, pyrrole-CH_3), 4.02 (m, 8 H, -CH_2CH$_3$), 7.37 (m, 3 H, ArH), 7.56 (m, 6 H, ArH), 7.62 (d, ^3J = 8 Hz, 2 H, ArH), 7.70 (d, ^3J = 8 Hz, 2 H, ArH), 7.82 (t, ^4J = 2 Hz, 1 H, ArH), 7.94 (m, 4 H, ArH), 8.11 (d, ^3J = 8 Hz, 2 H, ArH), 10.20 (s, 2 H, *meso*) ppm. HRMS (FAB) calcd. for $[C_{76}H_{72}N_4Zn]^+$: 1104.5048; found: 1104.5050.

ZnP-5B: Prepared from **ZnP-1B-I** (100 mg, 0.107 mmol) and **ethynyl-4B** (80 mg, 0.200 mmol) as described for **ZnP-ethynyl-3B-TIPS** and gave **ZnP-5B** as a red solid (18 mg, 0.007 mmol, 14%); ^{1}H NMR ($CDCl_3$): δ = 1.50 (s, 18 H, *t*Bu), 1.82 (m, 12 H, -CH_2CH_3), 2.64 (m, 12 H, pyrrole-CH_3), 4.04 (m, 8 H, -CH_2CH$_3$), 7.42–7.52 (m, 13 H, ArH), 7.56 (d, ^3J = 8 Hz, 2 H, ArH), 7.64 (d, ^3J = 8 Hz, 2 H, ArH), 7.95 (m, 3 H, ArH), 8.04 (m, 4 H, ArH), 10.35 (s, 2 H, *meso*) ppm. HRMS (FAB) calcd. for $[C_{84}H_{76}N_4Zn]^+$: 1204.5361; found: 1204.5375.

Supporting Information (see also the footnote on the first page of this article): ^{13}C NMR spectra and high-resolution mass spectrometry data for all new compounds are available. The observed data are all in good agreement with what is to be expected.

Acknowledgments

This work was supported by grants from the Swedish Research Council.

[1] T. Förster, *Naturwiss.* **1946**, *33*, 166–175.
[2] D. L. Dexter, *J. Chem. Phys.* **1953**, *21*, 836–850.
[3] H. M. McConnell, *J. Chem. Phys.* **1961**, *35*, 508–515.
[4] H. E. Zimmerman, T. D. Goldman, T. K. Hirzel, S. P. Schmidt, *J. Org. Chem.* **1980**, *45*, 3933–3951.
[5] H. Oevering, J. W. Verhoeven, M. N. Paddon-Row, E. Cotsaris, N. S. Hush, *Chem. Phys. Lett.* **1988**, *143*, 488–495.
[6] T. A. Smith, N. Lokan, N. Cabral, S. R. Davies, M. N. Paddon-Row, K. P. Ghiggino, *J. Photochem. Photobiol. A* **2002**, *149*, 55–69.
[7] A. Osuka, N. Tanabe, S. Kawabata, I. Yamazaki, Y. Nishimura, *J. Org. Chem.* **1995**, *60*, 7177–7185.
[8] H. S. Cho, D. H. Jeong, M.-C. Yoon, Y. H. Kim, Y.-R. Kim, D. Kim, S. C. Jeoung, S. K. Kim, N. Aratani, H. Shinmori, A. Osuka, *J. Phys. Chem. A* **2001**, *105*, 4200–4210.
[9] B. Schlicke, P. Belser, L. De Cola, E. Sabbioni, V. Balzani, *J. Am. Chem. Soc.* **1999**, *121*, 4207–4214.
[10] F. Barigelletti, L. Flamigni, M. Guardigli, A. Juris, M. Beley, S. Chodorowski-Kimmes, J.-P. Collin, J.-P. Sauvage, *Inorg. Chem.* **1996**, *35*, 136–142.
[11] A. Harriman, R. Ziessel, *Chem. Commun.* **1996**, 1707–1716.
[12] A. Harriman, A. Khatyr, R. Ziessel, A. C. Benniston, *Angew. Chem. Int. Ed.* **2000**, *39*, 4287–4290.
[13] J. Kroon, A. M. Oliver, M. N. Paddon-Row, J. W. Verhoeven, *J. Am. Chem. Soc.* **1990**, *112*, 4868–4873.
[14] K. Kilså, J. Kajanus, J. Mårtensson, B. Albinsson, *J. Phys. Chem. B* **1999**, *103*, 7329–7339.

[15] Previously reported to be 25.3 Å but more refined methods (DFT B3LYP/6-31G*) estimates the centre-to-centre distance to be 26.5 Å, see ref.[16].
[16] M. P. Eng, T. Ljungdahl, J. Mårtensson, B. Albinsson, *J. Phys. Chem.* in press.
[17] O. Lavastre, L. Ollivier, P. H. Dixneuf, S. Sibandhit, *Tetrahedron* **1996**, *52*, 5495–5504.
[18] J. Kajanus, S. B. van Berlekom, B. Albinsson, J. Mårtensson, *Synthesis* **1999**, 1155–1162.
[19] O. Lavastre, S. Cabioch, P. H. Dixneuf, J. Vohlidal, *Tetrahedron* **1997**, *53*, 7595–7604.
[20] H.-F. Chow, C.-W. Wan, K.-H. Low, Y.-Y. Yeung, *J. Org. Chem.* **2001**, *66*, 1910–1913.
[21] S. Misumi, *Bull. Chem. Soc. Jpn.* **1961**, *34*, 1827–1832.
[22] H. L. Anderson, J. K. M. Sanders, *J. Chem. Soc. Chem. Commun.* **1989**, 1714–1715.
[23] R. W. Wagner, T. E. Johnson, F. Li, J. S. Lindsey, *J. Org. Chem.* **1995**, *60*, 5266–5273.
[24] K. Pettersson, A. Kyrychenko, E. Rönnow, T. Ljungdahl, J. Mårtensson, B. Albinsson, *J. Phys. Chem. A* **2006**, *110*, 310–318.
[25] K. K. Jensen, S. B. van Berlekom, J. Kajanus, J. Mårtensson, B. Albinsson, *J. Phys. Chem. A* **1997**, *101*, 2218–2220.
[26] A. A. Bothner-By, J. Dadok, T. E. Johnson, J. S. Lindsey, *J. Phys. Chem.* **1996**, *100*, 17551–17557.
[27] J. Andréasson, J. Kajanus, J. Mårtensson, B. Albinsson, *J. Am. Chem. Soc.* **2000**, *122*, 9844–9845.
[28] C. Liang, M. D. Newton, *J. Phys. Chem.* **1992**, *96*, 2855–2866.
[29] J.-S. Hsiao, B. P. Krueger, R. W. Wagner, T. E. Johnson, J. K. Delaney, D. C. Mauzerall, G. R. Fleming, J. S. Lindsey, D. F. Bocian, R. J. Donohoe, *J. Am. Chem. Soc.* **1996**, *118*, 11181–11193.

Received: March 19, 2006
Published Online: May 12, 2006

